Journal of Power Sources 198 (2012) 127–131

Contents lists available at SciVerse ScienceDirect

Journal of Power Sources

journal homepage: www.elsevier.com/locate/jpowsour

Short communication

Highly catalytic activity of Pt electrocatalyst supported on sulphated SnO_2/multi-walled carbon nanotube composites for methanol electro-oxidation

Dao-Jun Guo, Jin-Mao You*

The Key Laboratory of Life-Organic Analysis, School of Chemistry and Chemical Engineering, Qufu Normal University, Qufu, Shandong 273165, PR China

ARTICLE INFO

Article history:
Received 30 July 2011
Received in revised form 5 October 2011
Accepted 6 October 2011
Available online 13 October 2011

Keywords:
Electrocatalyst
Solid superacid
Methanol oxidation
Proton conductivity
Direct methanol fuel cell

ABSTRACT

Highly catalytic active platinum nanoparticles supported on sulphated SnO_2/multi-walled carbon nanotube composites (Pt–S–SnO_2/MWCNT) are reported. As a novel catalyst support, S–SnO_2/MWCNT composites with both electron and proton conductivity can improve the catalytic activity and utilization of Pt catalyst in direct methanol fuel cell. X-ray diffraction and transmission electron microscopy show that the sulphated SnO_2 and Pt nanoparticle is coexist in the Pt–S–SnO_2/MWCNT composites and coated uniformly on the surface of the MWCNTs. Fourier transform infrared spectroscopy analysis proves that the MWCNT surfaces are modified with sulphated SnO_2 and a high concentration of SO_x, and adsorbed OH species exist on the surface of the sulphated SnO_2. Electrochemical studies are carried out using cyclic voltammetry, chronoamperometry and CO stripping voltammetry. The results indicate that Pt–S–SnO_2/MWCNT catalysts have much higher catalytic activity and CO tolerance for methanol electrooxidation than Pt-SnO_2/MWCNTs, commercial Pt/C and PtRu/C.

1. Introduction

Direct methanol fuel cells (DMFCs) are very promising, as they are capable of delivering high-power density at low and intermediate temperatures. The basic function of DMFCs involves the cathodic reduction of oxygen and anodic oxidation of methanol [1–3]. The precious metal Pt-based electrocatalysts are widely used for the anodic and cathodic reactions [4–11]. However, the major concerns with Pt-based catalyst is that catalyst poisoning during the anode reaction due to the adsorption of CO-like intermediates [4,7,12]. The high overpotential for the electrode reaction and poisoning of the catalyst significantly reduces the efficiency of fuel cell. On the other hand, the high cost of Pt-based catalyst is a barrier in the large scale commercialization of DMFCs. For the successful commercialization of such devices at low cost, the amount of Pt catalyst should be reduced significantly without sacrificing the efficiency of the device. The performance of DMFCs can be improved by (i) using nanosized Pt-based electrocatalysts and (ii) facilitating the easy accesses of the catalyst to the reactants. As a consequence, extensive efforts have been directed toward improving the CO tolerance and reducing Pt loading while maintaining high mass current density. Another important consideration is the enhancement of catalytic activity for methanol oxidation coupling with the decrease of catalyst cost which still presents an ongoing challenge in the development of practical DMFCs.

Up to now, many studies have shown that Pt-based catalysts decorated with metal oxides such as RuO_2–IrO_2 [13], MgO [14], CeO_2 [15], WO_3 [16], TiO_2 [17], ZrO_2 [18], and SnO_2 [19] have significant promotion effect on the catalytic activity and stability for the methanol oxidation reactions. However, metal oxide is semiconducting and has low electric conductivity. The Pt nanoparticles deposited on the surface of a thicker metal oxide layer or larger metal oxide particles, which may be useless due to poor conductivity. On the other hand, the large metal oxide particles with small surface area usually result in the poor dispersion of Pt nanoparticles. Therefore, an ideal support with high electron and proton conductivity is required not only to improve the catalytic activity, but also increase the utilization of Pt catalysts.

Sulphated SnO_2, also known as SO_4^{2-}–SnO_2 solid superacid, has relatively small particle size, high proton conductivity and good hydrophilic capacity due to the SO_4^{2-} group on the SnO_2 surface [20,21]. It is considered an ideal co-catalyst for methanol electrooxidation. In recent years, carbon nanotubes (CNTs) have attracted special attention as catalyst supports in fuel cell applications owing to their unique properties, such as large surface areas, high chemical resistivity, and superior mechanical strength. In addition, the hairlike structure of CNTs allows for entanglements among nanotubes, enabling better electron conductivity than traditional carbon systems [22]. So when mixed with CNT and solid superacid, it can be an ideal support for Pt catalyst in DMFCs, because the mixed-conducting materials combining a proton

* Corresponding author. Tel.: +86 0537 4458501; fax: +86 0537 4456305.
E-mail address: jmyou6304@163.com (J.-M. You).

0378-7753/$ – see front matter © 2011 Elsevier B.V. All rights reserved.
doi:10.1016/j.jpowsour.2011.10.017

conductor and an electron conductor. Thus, they can transport protons and electrons at the same time.

Herein we developed a kind of novel and efficient electrocatalyst, sulphated SnO_2 modified multi-walled carbon nanotubes composites as a new support of Pt catalysts (Pt–S–SnO_2/MWCNTs), for methanol oxidation. The special catalyst structure will increase the catalytic activity and utilization of Pt catalysts due to the high proton conductivity of sulphated SnO_2 and electron conductivity of CNTs. The materials were characterized by Fourier transform infrared spectroscopy (FTIR), X-ray diffraction (XRD), high-resolution transmission electron microscopy (HRTEM). Cyclic voltammetry (CV), chronoamperometry and impedance spectroscopy were used to evaluate their catalytic activities and durability for methanol oxidation.

2. Experimental

2.1. Synthesis of S–SnO_2/MWCNT supported Pt (Pt–S–SnO_2/MWCNT) electrocatalyst

For preparing S–SnO_2/MWCNT composites, multi-walled carbon nanotubes, hydrous tin(II) chloride ($SnCl_2{\cdot}2H_2O$), ammonia (NH_3) and sulphuric acid (H_2SO_4) were used as the starting material, precipitating agent and sulphating agent, respectively. Twenty-eight percent NH_3 aq. was gradually dropped into $SnCl_2{\cdot}2H_2O$ solution (0.20 M) with appropriate amounts of MWCNTs and the mixture was adjusted to pH 10, the mixture was stirred for 24 h. Then the obtained $SnO_2{\cdot}nH_2O$ sol was washed with distilled water using centrifuge till chloride ions were not detected by silver nitrate ($AgNO_3$), dried at 110 °C for 24 h and ground. The $SnO_2{\cdot}nH_2O$ and MWCNT composites were added to 0.50 M H_2SO_4 with vigorously stirring for 15 min, then was filtrated and dried at 90 °C. After that, the powder was calcinated at 550°C under N_2 flow for 1 h, the S–SnO_2/MWCNT supports thus prepared is denoted as S–SnO_2/MWCNTs, the S–SnO_2 content was 50% by weight in the catalyst supports. For comparison, the SnO_2/MWCNT composites were also obtained with the same process without H_2SO_4 added.

Afterwards, S–SnO_2/MWCNT powder and appropriate amounts of hexachloroplatinic acid hydrate ($H_2PtCl_6{\cdot}6H_2O$) were dispersed in 50 mL Millipore water to prepare a suspended solution. A freshly prepared solution of $NaBH_4$ was added dropwise into the above solution under vigorous stirring. After 30 min, the product is collected by centrifugation, washed several times with H_2O and ethanol, the obtained catalyst was dried in a vacuum oven at 70 °C overnight, then the 20 wt% Pt loading on the S–SnO_2/MWCNT support catalysts was obtained denoted as Pt–S–SnO_2/MWCNT. For comparison, Pt–SnO_2/MWCNT composites with the same contents of Pt were also obtained directly by reducing the Pt precursor in SnO_2/MWCNT suspension using the addition of $NaBH_4$ at room temperature.

2.2. Measurement

Electrochemical reactivity of the catalysts was measured by cyclic voltammetry (CV) using a three-electrode cell at the PARSTAT 2273 potentiostat controlled by PowerSuite® software (Princeton Applied Research). The working electrode was a gold plate covered with a thin layer of Nafion-impregnated catalyst. As a typical process, the catalyst ink was prepared by ultrasonically dispersed about 1 mg catalyst in the 25 μL mixture of Nafion solution (20% Nafion and 80% ethylene glycol) for 30 min. After casting the catalysts ink onto a polished planar gold patch (1.0 cm × 1.0 cm), the electrodes were air-dried at 80 °C for 1 h. Pt gauze and a saturated calomel electrode (SCE) were used as counter electrode and reference electrode, respectively. All potentials in this report are quoted versus SCE. CV test was conducted at 50 mV s^{-1} in a solution of 1 M $HClO_4$ with 1 M CH_3OH, potential ranging from −0.2 to 1.0 V. The oxidation of pre-adsorbed CO was measured by CO stripping voltammetry at a scan rate of 20 mV s^{-1}. All the electrochemical measurements were conducted under 25 °C.

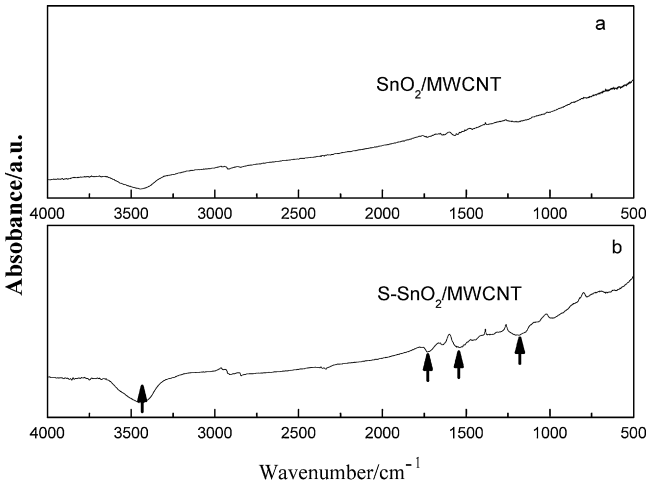

Fig. 1. FT-IR spectroscopy of S–SnO_2/MWCNT (a) and SnO_2/MWCNT (b) composites.

The morphology of Pt–S–SnO_2/MWCNT composites were investigated using high-resolution transmission electron microscopy (HRTEM, JEOL model JEM-2100) operated at 200 kV. The XRD patterns of the as-prepared products were investigated via a Bruker powder diffraction system (model D8 Advanced), using Cu K_α as the radiation source at the operating voltage of 40 kV and a scan rate of 6° min^{-1}. The FT-IR spectra were recorded in the range of 4000–400 cm^{-1} on a Spectrometer (GX FT-IR, Perkin Elmer, CA, USA), equipped with a DTGS detector. Each spectrum was an average of accumulation of 32 scans at a resolution of 4 cm^{-1}. The EDS analysis was carried out at 150 kV using an OXFORD INCA 300 energy dispersive X-ray spectrometer attached to a scanning electron microscope.

3. Results and discussion

3.1. IR spectra analysis of the S–SnO_2/MWCNT composites

Infrared spectra of S–SnO_2/MWCNT and SnO_2/MWCNT composites are illustrated in Fig. 1. The spectra were used to investigate the structure of sulphur on SnO_2 nanoparticles. Several absorption peaks in the 800–1300 cm^{-1} region were observed in the spectrum of the S–SnO_2/MWCNTs, but not in the spectrum of the SnO_2/MWCNTs. In Fig. 1a, the broad peaks between 800 cm^{-1} and 1300 cm^{-1} assigned to the S=O or S–O stretching frequency are the characteristic peaks. For S–SnO_2/MWCNT samples, S–SnO_2 nanoparticles are nanometer, so the fine structure splitting of IR spectra disappears, only broad bands between 1300 and 800 cm^{-1} showed attributing to the sulphated vibrational modes. This implies the presence of high-concentration SO_x bonded tightly with Sn, which leads to a high proton conductivity [23,24]. The strong and broad band detected in the region of 3200–3600 cm^{-1} and the weak peak at around 1631 cm^{-1} in curve (b) of Fig. 1 can be assigned to the deformation vibration mode of the adsorbed water [25]. It is well known that the oxidation of CO requires an adsorbed OH species adjacent to the adsorbed CO. Sulphated SnO_2 can adsorb and dissociate more water than non-sulphated SnO_2, which produces more hydroxyl groups. Thus the CO_{ads} on the surface of Pt during the methanol oxidation are much easier to be oxidized according

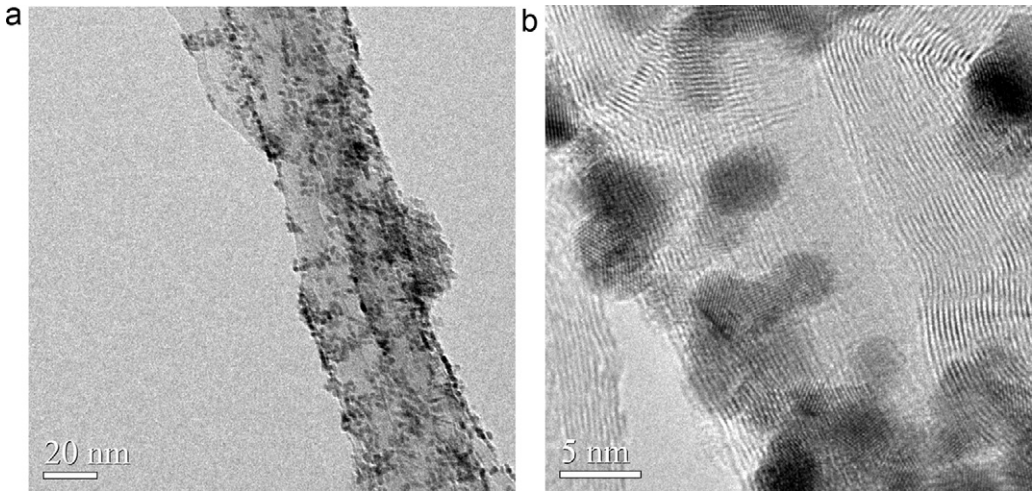

Fig. 2. TEM and HRTEM images of Pt–S–SnO_2/MWCNT composites.

to the bifunctional mechanism [26], releasing the active sites of Pt for further electrochemical reaction [27].

3.2. TEM analysis of the Pt–S–SnO_2/MWCNT composites

Fig. 2 shows the typical TEM and HRTEM images of the Pt–S–SnO_2/MWCNT composites. It can be seen from low-resolution TEM image that the Pt and S–SnO_2 nanoparticles are homogeneously dispersed on the sidewalls of the MWCNTs without aggregation. The HRTEM micrograph reveals further that Pt and S–SnO_2 nanoparticles attached on the sidewalls of the MWCNTs and the coating is rather uniform and thin, the diameter of the Pt particles is about only 2–6 nm with a mean value of 3.0 nm. Pt and S–SnO_2 nanoparticles can be easily identified from the crystal lattice pattern. The presence of Pt and S–SnO_2 nanoparticles can be further confirmed in the XRD results discussed as the following. Thus, two-dimensional Pt–S–SnO_2/MWCNT composites were obtained by using MWCNT as support materials. Because of high proton conductivity of sulphated SnO_2, those Pt catalysts deposited on S–SnO_2 surface can also been used for methanol electro-oxidation increasing the utilization of Pt catalyst.

The elemental composition of the Pt–S–SnO_2/MWCNT composites was characterized by EDS and the corresponding results are shown in Fig. 3. It can be observed that on the Pt–S–SnO_2/MWCNT electrodes, Pt, S, Sn, O and C are the major elements, which confirm that Pt and S–SnO_2 were dispersed on the MWCNT surface.

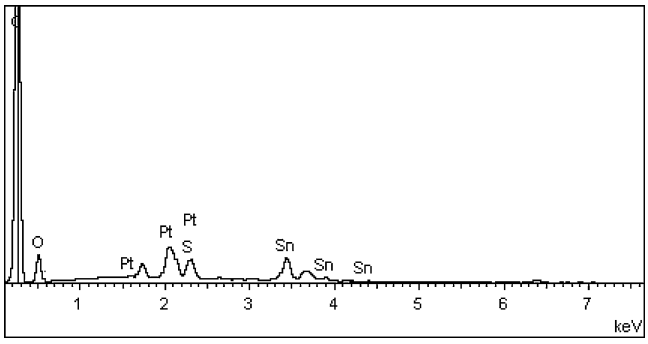

Fig. 3. EDS patterns of the Pt–S–SnO_2/MWCNT composites.

3.3. XRD analysis of the Pt–S–SnO_2/MWCNT composites

Fig. 4 shows the XRD patterns of Pt–S–SnO_2/MWCNTs and S–SnO_2/MWCNTs compared with Pt–SnO_2/MWCNTs and SnO_2/MWCNTs. The diffraction peaks of Pt, S–SnO_2 can be observed in the patterns of Pt–S–SnO_2/MWCNTs catalysts, indicating their coexistence in the samples. The diffraction peaks at ca. 40°, 46°, 68°, and 81° can be ascribed to the (1 1 1), (2 0 0), (2 2 0), and (3 1 1) planes of the face-centered cubic (fcc) structure of platinum. And there is no shift in any of the diffraction peaks of platinum in the Pt–S–SnO_2/MWCNTs and Pt–SnO_2/MWCNT catalysts, indicating that the addition of S–SnO_2 and SnO_2 has no effect on the crystalline lattice of platinum. The other phase showed a diffraction peak at around 26°, which is related to the crystalline nature of the graphitic structure of the CNTs. The diffraction peaks at ca. 34°, 53°, and 66° in the XRD patterns of S–SnO_2/MWCNTs and SnO_2/MWCNTs can be attributed to the (1 0 1), (2 1 1) and (3 0 1) faces of tetragonal SnO_2, respectively. The breadth of the XRD peaks also indicated that small Pt and S–SnO_2 crystallites were obtained. The average crystallite size of Pt nanoparticles calculated from the Pt (2 2 0) reflection plane by using the Debye–Scherrer equation was about 2.8 nm, in good agreement with the values obtained by HRTEM analysis.

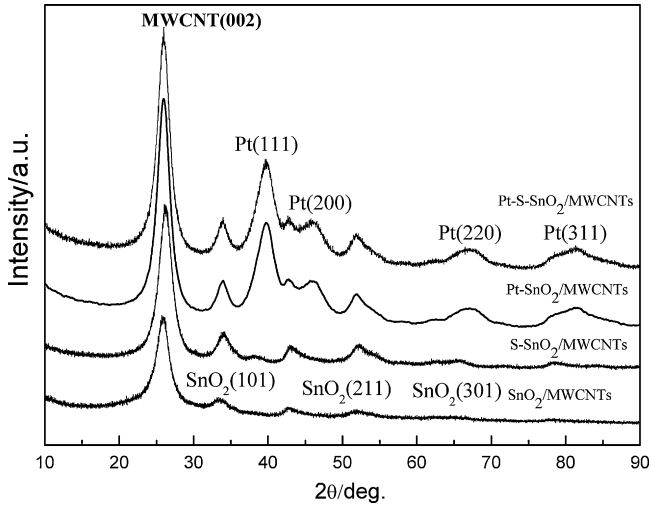

Fig. 4. XRD analysis of Pt–S–SnO_2/MWCNT, S–SnO_2/MWCNT and SnO_2/MWCNT composites.

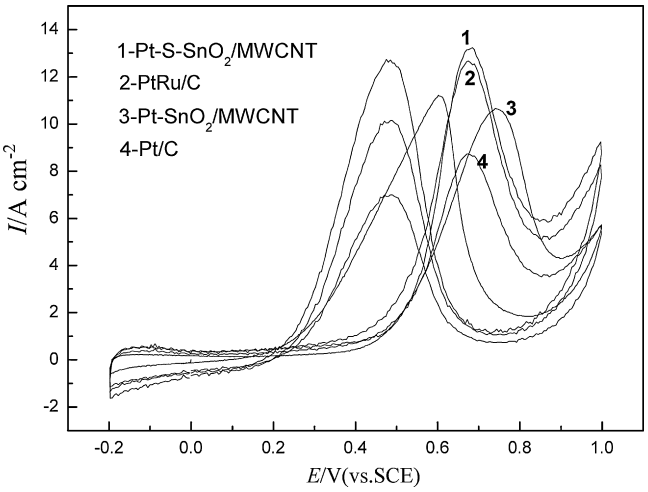

Fig. 5. Cyclic voltammograms of various electrodes at a scan rate of 50 mV s^{-1} in 1.0 M $HClO_4$ + 1.0 M CH_3OH aqueous solution.

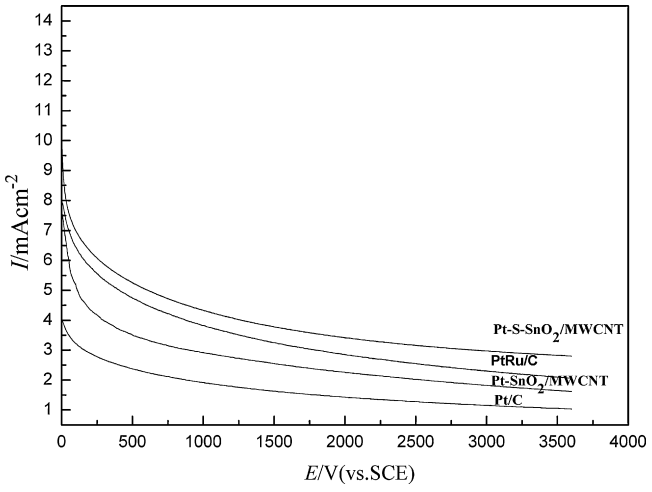

Fig. 6. Chronoamperograms of various electrodes at 0.45 V in 1.0 M $HClO_4$ + 1.0 M CH_3OH aqueous solution.

3.4. Electrochemical properties of Pt–S–SnO_2/MWCNT composites

The electrochemical properties of Pt–S–SnO_2/MWCNT compared with Pt–SnO_2/MWCNT, and commercial Pt/C (E-TEK) catalysts have been investigated by CV in 1 M $HClO_4$ and 1.0 M CH_3OH aqueous solutions and the corresponding CVs are shown in Fig. 5. The typical CVs of methanol oxidation can be observed on both electrodes. From Fig. 5, it can clearly be seen that the current density of the Pt–S–SnO_2/MWCNTs catalyst is higher than that of the Pt–SnO_2/MWCNTs and commercial Pt/C catalyst. The peak current densities obtained at the potential of about 0.7 V in the forward scan for Pt–S–SnO_2/MWCNTs, PtRu/C, Pt–SnO_2/MWCNTs and Pt/C catalysts are 13.16 A cm^{-2}, 12.6 A cm^{-2}, 10.6 A cm^{-2} and 8.7 A cm^{-2}, respectively. The Pt–S–SnO_2/MWCNT catalyst displays a current density 1.24 times higher than that of the Pt–SnO_2/MWCNTs, 1.1 and 1.51 times than commercial PtRu/C and Pt/C catalysts. The onset potential in the positive direction of methanol oxidation on the Pt–S–SnO_2/MWCNTs was 0.24 V, which is lower than the PtRu/C (0.25 V), Pt–SnO_2/MWCNT (0.26 V) and Pt/C (0.28 V) catalysts. Current density and onset potential of methanol oxidation are two important parameters to evaluate the performance of electro-catalysts. The lower onset potential and higher peak current density of methanol oxidation indicate higher catalytic activity of Pt-based catalyst. Sulphated SnO_2 is a proton conductor and can dissociate H_2O under lower potentials than SnO_2 with had been discussed in the FTIR section to supply OH_{ads} for CO oxidation produced during the methanol oxidation on the surface of Pt, as a support for a Pt catalyst it may facilitate the utilization of the catalyst for methanol oxidation.

The catalytic activities and stability of Pt–S–SnO_2/MWCNT compared with Pt–SnO_2/MWCNT and commercial PtRu/C, Pt/C catalysts for methanol oxidation has also been investigated by chronoamperometric tests and the corresponding curves are shown in Fig. 6. As shown, at 0.45 V the initial current densities of the Pt–S–SnO_2/MWCNT were significantly higher than those of the Pt-SnO_2/MWCNT and PtRu/C, Pt/C catalysts indicating the higher double-layer charging. In general, methanol was continuously oxidized on the catalyst surface when the potential was fixed at 0.45 V, many reaction intermediate species such as adsorbed CO would begin to accumulate on the surface of Pt catalysts during the oxidation of methanol. In general, if the kinetics of the removal for intermediate species is poor, the decreases of the current density will be fast, a gradual decay of current density with time implies that the catalyst has good anti-poisoning ability. The current decayed more slowly for the Pt–S–SnO_2/MWCNT than the two others catalysts indicating less accumulation of adsorbed CO species. This implies that the Pt–S–SnO_2/MWCNT composite exhibits higher catalytic activity and better stability than the PtRu/C, Pt–SnO_2/MWCNT and Pt/C composite.

All the above CV and chronoamperometry results indicate that the Pt–S–SnO_2/MWCNT catalyst exhibits higher catalytic activity and CO tolerance for methanol oxidation than the Pt–SnO_2/MWCNTs and Pt/C catalyst. Since CO species are the main poisoning intermediate, a good catalyst for methanol electro-oxidation should possess excellent CO electro-oxidizing ability, which can be reflected from CO stripping test. We compared the three catalysts in terms of CO eliminating ability. The CO stripping voltammogram curves were shown in Fig. 7. Much more differences are observed in the onset potential and peak potential of CO oxidation. The onset potential for the Pt–S–SnO_2/MWCNTs was at 0.31 V, which was about 0.1 V lower than that measured on the Pt–SnO_2/MWCNT electrode (0.41 V), showing that the addition of sulphated SnO_2 is more beneficial for CO electrooxidation than SnO_2 alone. The highest onset potential (0.51 V) was found on the Pt/C electrode. The peak potentials of CO oxidation showed the same order as the onset potentials: Pt–S–SnO_2/MWCNTs (0.44 V) < Pt–SnO_2/MWCNTs (0.50 V) < Pt/C (0.59 V). These results demonstrate that CO can be oxidized more

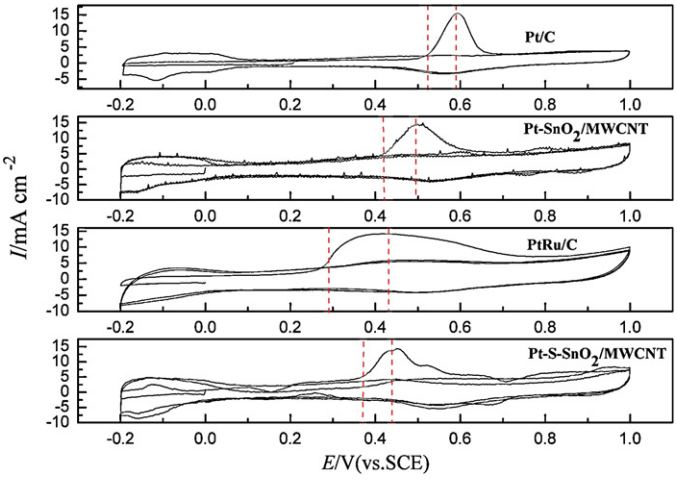

Fig. 7. CO stripping curves of various electrodes at a scan rate of 20 mV s^{-1} in 1 M $HClO_4$.

easy on Pt–S–SnO_2/MWCNTs electrode than on Pt–SnO_2/MWCNTs and Pt/C electrodes. This can be attributed to the presence of more absorbed OH (OH_{ads}) on the S–SnO_2/MWCNT supports with is favourable for bifunctional mechanism. But compared with PtRu/C catalysts, the onset potential (0.29 V at PtRu/C) and peak potential (0.43 V at PtRu/C) of CO stripping at Pt–S–SnO_2/MWCNT catalysts are higher than that of PtRu/C, the results show that OH can be easily formed at the Ru surface, but as well known that Ru can be easily dissolved during the oxidation of methanol, so the Pt–S–SnO_2/MWCNT catalysts are more stable than that of PtRu/C catalysts and can be used as potential catalysts in the direct methanol fuel cell.

4. Conclusions

A novel structurally controlled Pt–S–SnO_2/MWCNT catalyst was prepared for direct methanol fuel cell in the presented work. TEM and XRD show that the Pt nanoparticles were uniformly dispersed on the sulphated SnO_2-coated MWCNTs. FT-IR analysis indicated that SO_x and OH_{ads} also existed on the surface of the sulphated SnO_2. Electrochemical studies using chronoamperometry, cyclic voltammetry and CO stripping voltammetry found that the structure of the catalyst and a larger amount of OH_{ads} increased the synergetic interaction between Pt and sulphated SnO_2. The high electron and proton conductivities of the Pt–S–SnO_2/MWCNT composite increased the rate and current density of methanol oxidation and the utilization of Pt catalysts. All these results reveal that the prepared catalyst is a promising anode catalyst for DMFC.

Acknowledgements

This project was supported by the Excellent Middle-age and Young Scientists Research Award Foundation of Shandong Province (BS2010NJ008), the Provincial Natural Science Foundation of Shandong Province (ZR2010BM010, ZR2010BL013) and the Scientific Research Foundation of Qufu Normal University (BSQD09069).

References

[1] K.V. Kordesch, G.R. Simader, Environmental impact of fuel cell technology, Chem. Rev. 95 (1995) 191–207.
[2] L. Carrette, K.A. Friedrch, U. Stimming, Fuel cells: principles types, fuels, and applications, ChemPhysChem 1 (2000) 163–193.
[3] C.Y. Wang, Fundamental models for fuel cell engineering, Chem. Rev. 104 (2004) 4727–4765.
[4] N.M. Markovic, H.A. Gasteiger, P.N. Ross Jr., Oxygen reduction on platinum low-index single-crystal surfaces in sulphuric acid solution: rotating ring–Pt(hkl) disk studies, J. Phys. Chem. 99 (1995) 3411–3415.
[5] B. Lim, M. Jiang, P.H.C. Camargo, E.C. Cho, J. Tao, X. Lu, Y. Zhu, Y. Xia, Pd–Pt bimetallic nanodendrites with high activity for oxygen reduction, Science 324 (2009) 1302–1305.
[6] M.H. Shao, T. Huang, P. Liu, J. Zhang, K. Sasaki, M.B. Vukmirovic, R.R. Adzic, Palladium monolayer and palladium alloy electrocatalysts for oxygen reduction, Langmuir 22 (2006) 10409–10415.
[7] K. Kinoshita, Electrochemical Oxygen Technology, John Wiley &Sons, Inc., New York, 1992, p. 307.
[8] G. Chang, M. Oyama, K. Hirao, Seed-mediated growth of palladium nanocrystals on indium tin oxide surfaces and their applicability as modified electrodes, J. Phys. Chem. B 110 (2006) 20362–20368.
[9] Y. Lou, M.M. Maye, L. Han, J. Luo, C.J. Zhong, Gold–platinum alloy nanoparticle assembly as catalyst for methanol electrooxidation, Chem. Commun. 7 (2001) 3–474.
[10] E.P. Lee, Z. Peng, W. Chen, S. Chen, H. Yang, Y. Xia, Electrocatalytic properties of Pt nanowires supported on Pt and W gauzes, ACS Nano 2 (2008) 2167–2173.
[11] J. Zhang, Y. Mo, M.B. Vukmirovic, R. Klie, K. Sasaki, R.R. Adzic, Platinum monolayer electrocatalysts for O_2 reduction: Pt monolayer on Pd(1 1 1) and on carbon-supported Pd nanoparticles, J. Phys. Chem. B 108 (2004) 10955–10964.
[12] T.D. Jarvi, E.M. Stuve, in: J. Lipkowski, P.N. Ross (Eds.), Electrocatalysis, Wiley-VCH, New York, 1998, p. 75.
[13] M.L. Calegaro, H.B. Suffredini, S.A.S. Machado, L.A. Avaca, Preparation characterization and utilization of a new electrocatalyst for ethanol oxidation obtained by the sol–gel method, J. Power Sources 156 (2006) 300–305.
[14] C.W. Xu, P.K. Shen, X.H. Ji, R. Zeng, Y.L. Liu, Enhanced activity for ethanol electrooxidation on Pt–MgO/C catalysts, Electrochem. Commun. 7 (2005) 1305–1308.
[15] C.W. Xu, P.K. Shen, Electrochamical oxidation of ethanol on Pt–CeO_2/C catalysts, J. Power Sources 142 (2005) 27–29.
[16] D.Y. Zhang, Z.F. Ma, G. Wang, K. Konstantinov, X. Yuan, H.K. Liu, Electro-oxidation of ethanol on Pt–WO_3/C electrocatalyst, Electrochem. Solid State Lett. 9 (2006) A423–A426.
[17] H.Q. Song, X.P. Qiu, F.S. Li, W.T. Zhu, L.Q. Chen, Ethanol electro-oxidation on catalysts with TiO_2 coated carbon nanotubes as support, Electrochem. Commun. 9 (2007) 1416–1421.
[18] H. Song, X. Qiu, F. Li, Promotion of carbon nanotube-supported Pt catalyst for methanol and ethanol electro-oxidation by ZrO_2 in acidic media, Appl. Catal. A: Gen. 364 (2009) 1–7.
[19] L.H. Jiang, G.Q. Sun, Z.H. Zhou, S.G. Sun, Q. Wang, S.Y. Yan, H.Q. Li, J. Tian, J.S. Guo, B. Zhou, Q. Xin, Size-controllable synthesis of monodispersed SnO_2 nanoparticles and application in electrocatalysts, J. Phys. Chem. B 109 (2005) 8774–8778.
[20] H. Matsuhashi, H. Miyazaki, Y. Kawamura, H. Nakamura, K. Arata, Preparation of a solid superacid of sulphated tin oxide with acidity higher than that of sulphated zirconia and its applications to aldol condensation and benzoylation, Chem. Mater. 13 (2001) 3038–3042.
[21] H. Matsuhashi, H. Miyazaki, K. Arata, The preparation of solid superacid of sulphated tin oxide with acidity higher than sulphated zirconia, Chem. Lett. 30 (2001) 452–453.
[22] Y.L. Hsin, K.C. Hwang, C.T. Yeh, Poly(vinylpyrrolidone)-modified graphite carbon nanofibers as promising supports for PtRu catalysts in direct methanol fuel cells, J. Am. Chem. Soc. 129 (2007) 9999–10010.
[23] G. Colon, M.C. Hidalgo, G. Munuera, I. Ferino, M.G. Cutrufello, J.A. Navio, Structural and surface approach to the enhanced photocatalytic activity of sulphated TiO_2 photocatalyst, Appl. Catal. B: Environ. 63 (2006) 45–59.
[24] S. Hara, M. Miyayama, Proton conductivity of superacidic sulphated zirconia, Solid State Ionics 168 (2004) 111–116.
[25] X. Cui, H. Ma, B. Wang, H. Chen, Direct oxidation of n-heptane to ester over modified sulphated SnO_2 catalysts under mild conditions, J. Hazard. Mater. 147 (2007) 800–805.
[26] Y.X. Bai, J.J. Wu, X.P. Qiu, J.Y. Xi, J.S. Wang, J.F.G. Li, W.T. Zhu, L.Q. Chen, Electrochemical characterization of Pt–CeO_2/C and Pt–$Ce_xZr_{1-x}O_2$/C catalysts for ethanol electro-oxidation, Appl. Catal. B: Environ. 73 (2007) 144–149.
[27] X.W. Zhang, H. Zhu, Z.J. Guo, Y.S. Wei, F.H. Wang, Design and preparation of CNT@SnO_2 core–shell composites with thin shell and its application for ethanol oxidation, Int. J. Hydrogen Energy 35 (2010) 8841–8847.